Granular Matter 5, 91–98 © Springer-Verlag 2003
DOI 10.1007/s10035-003-0129-7

A discrete model of a two-particle contact applied to cohesive granular materials

Jacek S. Leszczynski

Abstract In this paper, we consider the complex problem of how to simulate particle contacts, taking into account the cohesion effect. In accordance with the molecular dynamics models, we propose a novel expression for the repulsive force which controls dynamically the transfer and dissipation of energy in granular media. This expression is formulated under fractional calculus, where a fractional derivative accumulates the whole history of the virtual overlap over time in weighted form. We then discuss and illustrate the basic properties of the repulsive force in a normal direction to the contacting surfaces. This approach allows us to perform simulations of arbitrary multiparticle contacts as well as granular cohesion dynamics.

Keywords Granular systems, Molecular dynamics models, Repulsive force, Multiparticle contacts, Cohesion, Fractional calculus, Riemann-Liouville derivative, Caputo derivative

1 Introduction

The dynamics of granular materials have recently attracted much interest from the physics and engineering communities. One of the major aspects which needs to be taken into account with this media is how to model correctly the interactions that may eventually take place between particles. The collision process is responsible for the transfer and dissipation of energy in granular materials. An understanding of the contact processes is, therefore, crucial in order to develop theoretical studies and also to perform simulations. In dry and lean granular systems we observe binary collisions between particles, whereas in dense granular media we can see multiparticle contacts. A more complex interaction process occurs when we analyse dense and cohesive systems. In all the considered cases, the contact processes are characterised through their collisional time. An infinitesimally short time is suitable for binary collisions. However, as the time increases and tends toward infinity we can observe a progression from multiparticle contacts through non-permanent cohesion in multiparticle contacts to permanent cohesion. Cohesion between contacting particles may arise from a variety of sources [26]. In this paper we consider this cohesion as being dependent on the roughness of contacting surfaces. In the natural flow of granular materials all the considered cases can be locally distinguished as existing either respectively or simultaneously. Consequently modelling such a flow is limited by the assumptions concerning the contact processes.

Continuum models [5] are strongly based on binary collisions. These models do not consider the discrete nature and anisotropic properties of the contacting materials. Discrete models [6,8,16], however, much better reflect the interaction process. In this paper, we will focus on the molecular dynamics models taking into account an expression for the repulsive force acting between particles. Particularly, we will analyse what happens in cohesive materials during multiparticle contacts when the contacting surfaces of particles are rough [9]. Multiparticle collisions occur when a particle interacts with surrounding particles. Basic molecular dynamics models [8,21] are only valid for particle contacts which are independent of one another. But in cohesive particles we can observe the opposite situation. Moreover, papers [12,20] have examined the lack of energy dissipation in molecular dynamics. This is based on an assumption that the repulsive force does not reflect real energy loss. In this paper, we shall generalise the repulsive force as being in a normal direction to the contacting surfaces. We will also investigate the properties of this force.

Let us consider to a set of spherical particles np moving under arbitrary extortion. The particles are indexed from 1 to np sequentially. We can describe a particle through its characteristic mass m_i, diameter d_i or radius r_i, inertia moment $\mathcal{I}_i$, position $\mathbf{x}_i$, linear speed $\dot{\mathbf{x}}_i$ and spin vector $\boldsymbol{\omega}_i$, for $i \in \{1, \ldots, np\}$, where np is the total number of considered particles. Let us consider the multiparticle contacts shown in Fig. 1. In this figure we focus on a particle i which collides with surrounding particles $j(i)$. We introduced the natural function $j(i)$ $(j(i) \neq i)$ of the index i in order to find the particle number of a particle in a set of particles. We cannot exclude the situation that the surrounding particles contact with other ones. Fig. 1 presents a group of colliding particles moving as one object. We can analyse the object's dynamics through the exchange of particles within the object. A set of equations describing particle motion can be written as

Received: 29 September 2002

Jacek S. Leszczynski
Institute of Mathematics & Computer Science
Technical University of Czestochowa
ul. Dabrowskiego 73, 42-200 Czestochowa, Poland
e-mail: jale@k2.pcz.czest.pl

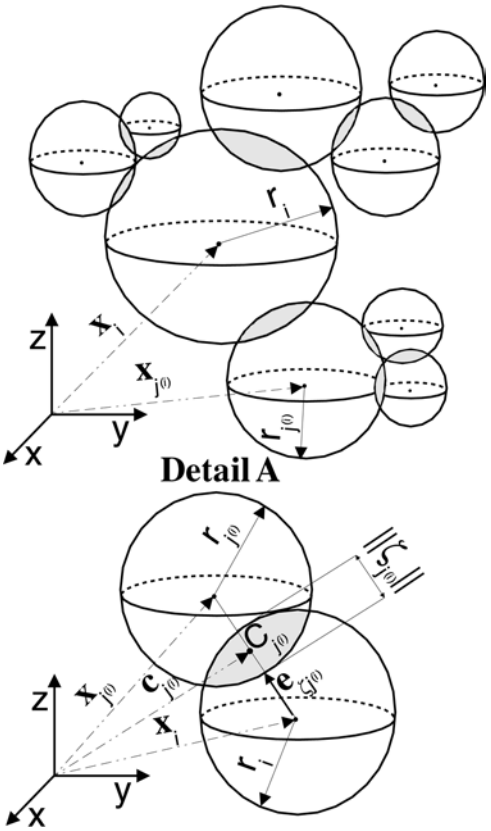

Fig. 1. Scheme illustrates multiparticle contacts

$$\begin{cases} m_i \cdot \ddot{\mathbf{x}}_i + \sum\limits_{j(i)} \sum\limits_{j(i)\neq i} \mathbf{P}_{j(i)} = \sum\limits_{l=1}^{nc} \mathbf{F}_l \\ \mathcal{I}_i \cdot \dot{\boldsymbol{\omega}}_i + \sum\limits_{j(i)} \sum\limits_{j(i)\neq i} \mathbf{s}_{j(i)} \times \mathbf{P}_{j(i)} = \sum\limits_{l=1}^{nc} \mathbf{M}_l \end{cases}, \tag{1}$$

where $\mathbf{F}_l$ is an optional force, $\mathbf{P}_{j(i)}$ denotes a repulsive force acting between a pair of colliding particles, $\mathbf{M}_l$ is an optional torque, nc is the total number of optional forces (torques) taken into account in our considerations, $\mathbf{s}_{j(i)}$ indicates the branch vector connecting the mass centre of particle i with the point of application of the repulsive force $\mathbf{P}_{j(i)}$. This point is defined as the centre of mass of the overlapping region which belongs to the contacting particles (see detail A in Fig. 1 and additional explanations given later). As the optional force we can distinguish gravitational force, drag force, etc. The repulsive force is defined according to molecular dynamics models. In such models particles virtually overlap when a contact occurs. According to [14,20] we define the overlap of two particles experiencing a contact as (see also detail A in Fig. 1)

$$\left\| \boldsymbol{\zeta}_{j(i)} \right\| = r_{j(i)} + r_i - \left\| \mathbf{x}_{j(i)} - \mathbf{x}_i \right\|, \tag{2}$$

and a normal unit vector $\mathbf{e}_{\zeta_{j(i)}}$ that connects the particles' centres of mass, pointing from i to $j(i)$, is

$$\mathbf{e}_{\zeta_{j(i)}} = \frac{\mathbf{x}_{j(i)} - \mathbf{x}_i}{\left\| \mathbf{x}_{j(i)} - \mathbf{x}_i \right\|}. \tag{3}$$

Eq. (1) shows the arbitrary motion of an individual particle which experiences a contact with neighbouring particles. If no contacts occur, the sum of repulsive forces (torques) in Eq. (1) is neglected. Solving over time t (an independent value) these two groups of equations one can find an explicit time $t^*_{j(i)}$ when a collision begins. This leads us to consider $\left\| \boldsymbol{\zeta}_{j(i)} \right\| = 0$.

Let $\mathbf{c}_{j(i)}$ be a position vector which is taken as the mass centre of the overlapping region as shown in detail A in Fig. 1. Taking into account the fact that the spherical particles interact only when their overlap (2) is positive, we have

$$\mathbf{c}_{j(i)} = \mathbf{x}_i + \left(r_i - \frac{\left\| \boldsymbol{\zeta}_{j(i)} \right\| \cdot \left(r_{j(i)} - \left\| \boldsymbol{\zeta}_{j(i)} \right\| \right)}{r_i + r_{j(i)} - \left\| \boldsymbol{\zeta}_{j(i)} \right\|} \right) \cdot \mathbf{e}_{\zeta_{j(i)}}. \tag{4}$$

In the case when a collision begins $\left(\left\| \boldsymbol{\zeta}_{j(i)} \right\| = 0 \right)$ we obtain

$$\mathbf{c}_{j(i)} = \frac{r_i \cdot \mathbf{x}_{j(i)} + r_{j(i)} \cdot \mathbf{x}_i}{r_{j(i)} + r_i}. \tag{5}$$

At a point created by the position vector (4) the contact force is applied. This notation allows us to consider multiparticle contacts where a particle i collides with surrounding particles $j(i)$. Therefore a few overlaps and normal unit vectors indexed $j(i)$ on the particle i may occur. From Eqs (2), (3) a vector of the normal overlap reads

$$\boldsymbol{\zeta}_{j(i)} = \left(r_{j(i)} + r_i \right) \cdot \mathbf{e}_{\zeta_{j(i)}} - \left(\mathbf{x}_{j(i)} - \mathbf{x}_i \right). \tag{6}$$

Only central collisions are considered in this paper. This means that the contact force acts in the normal direction ($\mathbf{P}_{j(i)} = \mathbf{P}_{\zeta_{j(i)}}$), which connects the mass centres of the colliding particles. We neglect particle rotation by assuming $\boldsymbol{\omega}_i = \mathbf{0}$.

2
Schemes of a normal force in particle contacts

Here we present examples of the normal force models, i.e. those most frequently used for practical simulations. Cundall and Strack [3] proposed the force as being a linear combination of elastic and viscous terms

$$\mathbf{P}_{\zeta_{j(i)}} = c_{j(i)} \cdot \dot{\boldsymbol{\zeta}}_{j(i)} + k_{j(i)} \cdot \boldsymbol{\zeta}_{j(i)}, \tag{7}$$

where $k_{j(i)}$ is the stiffness of a spring whose elongation is the particle deformation $\boldsymbol{\zeta}_j(i)$ and $c_{j(i)}$ is a damping constant.

Kuwabara and Kono [11] extended the original Hertz contact theory and investigated a nonlinear version of Eq. (7) in the form

$$\mathbf{P}_{\zeta_{j(i)}} = c_{j(i)} \cdot \dot{\boldsymbol{\zeta}}_{j(i)} \cdot \left| \boldsymbol{\zeta}_{j(i)} \right|^{\frac{1}{2}} \cdot \operatorname{sign}\left(\boldsymbol{\zeta}_{j(i)} \right) + k_{j(i)} \cdot \left| \boldsymbol{\zeta}_{j(i)} \right|^{\frac{3}{2}} \cdot \operatorname{sign}\left(\boldsymbol{\zeta}_{j(i)} \right). \tag{8}$$

Walton and Braun [27] proposed the elastoplastic deformation. They assumed different spring constants, $k_{j(i)}$ for the loading part and $k^*_{j(i)}$ for the unloading part of the contact

$$\mathbf{P}_{\zeta_{j(i)}} = \begin{cases} k_{j(i)} \cdot \boldsymbol{\zeta}_{j(i)}, & \dot{\boldsymbol{\zeta}}_{j(i)} \geq 0 \text{ (load)} \\ k^*_{j(i)} \cdot \left(\boldsymbol{\zeta}_{j(i)} - \boldsymbol{\zeta}^*_{j(i)} \right), & \dot{\boldsymbol{\zeta}}_{j(i)} < 0 \text{ (unload)} \end{cases}, \tag{9}$$

where $\boldsymbol{\zeta}^*_{j(i)}$ is the value of $\boldsymbol{\zeta}_{j(i)}$ when the unloading curve intersects the permanent plastic deformation. These repulsive force models represent the basic laws of interaction of a two-particle contact between grains.

In multiparticle contacts, we need to take into account the sum of forces (7), (8) or (9) depending on the force schemes. It should be noted that formulae (7) (8) and (9) are not suitable for arbitrary multiparticle contacts. In the above interaction laws we assume that particle contacts are independent of one another. If no mutual dependencies occur during multiparticle contacts, the local collisional time considered between a pair of contacting particles does not change. Only the coefficients and initial conditions used in the interaction laws have direct influence on the contact time in a two-particle collision. Some analytical expressions concerning the collisional time can be found in [3,11,27]. In practical computations we assume coefficients $c_{j(i)}$ and $k_{j(i)}$ are functional expressions as shown in [20]. Particularly, they depend on a normal restitution coefficient and also on the collisional time. The restitution coefficient describes the work of deformation between contacting bodies but does not say how much time is required for particle collisions.

With regard to the behaviour of an "object" composed of particles, as shown in Fig. 1 and described in the previous section, we cannot analyse the real dynamics of object. When analysing the dynamics of multiparticle contacts we should take into account some variations in time for both the restitution coefficient and the collisional time. Obviously, this is a disadvantage when calculating the repulsive force according to the basic interaction laws. Moreover, the coefficients $c_{j(i)}$, $k_{j(i)}$ in those force models represent the viscoelastic properties of contacting granular materials but do not reflect the surface properties of the particles. In the real behaviour of granular materials we can easily change the surface properties of the colliding particles as they are independent of structural properties. This can be easily seen, when we consider the contacts in a granular material for smooth particles and for rough ones. Therefore we cannot perform simulations taking into account the dynamics of multiparticle contacts. Following on from on Luding et al [12] who observed anomalous energy dissipation. We can try to explain the anomalous using fractional calculus [7], which means that during multiparticle contacts we need to take into account the history of energy and momentum transfer between particles. At this crucial point in our considerations, we need to introduce *a memory process* during multiparticle collisions. We can say that a particle has to remember about surrounding particles during the collision process.

In this paper we assume that for a two-particle collision the contacting surfaces are rough. According to Johnson [9], the contact between rough surfaces is discontinuous and the real area of contact is a small fraction of the nominal contact area taken into account on smooth surfaces. Therefore, another form of energy transfer between colliding bodies should be considered. Linear (7) and non-linear (8) interaction laws present the sum of elastic and viscous terms as being independent of one another. Pöschel et al [19] noted that this feature is reflected by the smooth surfaces in a topological sense. Barabási et al [2] proposed fractal concepts to describe a rough surface. In paper [2], they discussed a roughness exponent α related to fractal dimension. The roughness exponent α, which characterises the roughness of a surface, behaves as $\sim t^{\alpha}$ in scaling dynamics of growth surfaces. Johnson [9] presented a definition and experimental evidence of the roughness coefficient α which is limited to the elastic contact between rough surfaces. The parameter α defined in [9] was used as a measure of the effect of surface roughness on static contact under a purely normal load. Moreover, several studies [2,4,10,18] have examined experimentally rough surfaces through the roughness exponent α in fractal sense. Note that fractional derivatives [7,22] may reflect the scaling dynamics $\sim t^{\alpha}$ as a memory process. Following on from the results presented above we noted that the behaviour of elastic and viscous energies during contact between rough surfaces is the sum of all local contact zones on the total area of the contact. Therefore, the total elastic and viscous sources considered within the overlapping region (2) depend on the roughness parameter α between two contacting surfaces. Bagley and Torvik [1] introduced the fractional model of viscoelastic behaviour, which employs derivatives of fractional order to relate stress fields to strain fields in viscoelastic materials. They assumed that the stress in a viscoelastic material is a function not only of the actual strain at the time instant of the deformation process, but also of the previous strain history. Schiessel et al [25] demonstrated a generalised model of viscoelastic materials realised physically through hierarchical arrangements of springs and dashpots, such as ladders, trees or fractal structures. In this model, the order α of the fractional derivative relates to a material parameter which can be associated with a degree of conversion as, for example, for molecular theories [1]. Experimental evidence of the parameter α can be found in [15,24].

Sumarising previous considerations and using results concerning the generalised viscoelastic model [25], and the description of the fractal concept [2], we formulate the normal force acting between a pair of particles in the following form

$$\mathbf{P}_{\zeta_{j(i)}} = c_{j(i)}^{\alpha_{j(i)}} \cdot k_{j(i)}^{1-\alpha_{j(i)}} \cdot {}_{t^*_{j(i)}}D^{\alpha_{j(i)}}_{t_{j(i)}}\left(\boldsymbol{\zeta}_{j(i)}\right), \tag{10}$$

where $c_{j(i)}$, $k_{j(i)}$ are dumping and stiffness coefficients, ${}_{t^*_{j(i)}}D^{\alpha_{j(i)}}_{t_{j(i)}}\left(\boldsymbol{\zeta}_{j(i)}\right)$ is a differential operator of fractional order $\alpha_{j(i)}$ [22] and $t^*_{j(i)}$ is the begin time of a contact which leads to an initial condition $\left\|\boldsymbol{\zeta}_{j(i)}\right\| = 0$. We introduce a definition of this operator as the left side Riemann-Liouville fractional derivative [22]

$${}_{t^*}D^{\alpha}_{t} f(t) = \begin{cases} \frac{1}{\Gamma(n-\alpha)} \cdot \frac{d^n}{d\,t^n} \int\limits_{t^*}^{t} \frac{f(\tau)}{(t-\tau)^{\alpha-n+1}} d\tau, \\ \qquad\qquad\qquad\qquad n-1 < \alpha < n \\ \frac{d^n}{d\,(t-t^*)^n} f\,(t)\,, \qquad\qquad \alpha = n \end{cases}, \tag{11}$$

where $n = [\alpha] + 1$ and $[\cdot]$ denotes an integer part of a real number. In comparison to derivatives of integer order, which depend only on the local behaviour of the function, derivatives of fractional order accumulate the whole history of a function. This is the *memory effect*. To take into account the fact [7] that the Riemann-Liouville derivative has no physical interpretation especially when it

introduces initial conditions, we introduce the Caputo derivative [22]

$$ {}_{t^*}^{C}D_t^{\alpha} f(t) = \begin{cases} \frac{1}{\Gamma(n-\alpha)} \cdot \int\limits_{t^*}^{t} \frac{\frac{d^n f(\tau)}{d\tau^n}}{(t-\tau)^{\alpha-n+1}} d\tau, \\ \qquad\qquad\qquad\qquad n-1 < \alpha < n \\ \frac{d^n}{d\,(t-t^*)^n} f\,(t)\,, \\ \qquad\qquad\qquad\qquad \alpha = n \end{cases} . \quad (12) $$

We also need to present the transition between these derivatives, and following on from [22] we have

$$ {}_{t^*}D_t^{\alpha} f(t) = \sum_{l=0}^{n-1} \frac{(t-t^*)^{l-\alpha}}{\Gamma\,(l-\alpha+1)} \cdot f^{(l)}\,(t^*) + {}_{t^*}^{C}D_t^{\alpha} f(t), \quad (13) $$

where the sum represents the initial conditions. We need to formulate transition (13) because, while many investigations have concentrated on the Riemann-Liouville derivative, there is a complete lack of physical applications.

With regard to Eq (10), we apply the fractional operator (13), which is composed of the initial conditions and the Caputo derivative (12). Note that this repulsive force accumulates the history of the overlap $\boldsymbol{\zeta}_{j(i)}$ from the begin time of a contact $t^*_{j(i)}$ to the actual time $t_{j(i)}$ when the contact is finished. This corresponds to the memory effect in viscoelastic materials presented by Bagley and Torvik [1]. Hence, the model operates on the following conditions: $\boldsymbol{\zeta}_{j(i)}\left(t^*_{j(i)}\right) = \mathbf{0}$, $\dot{\boldsymbol{\zeta}}_{j(i)}\left(t^*_{j(i)}\right) = \dot{\mathbf{x}}_i\left(t^*_{j(i)}\right) - \dot{\mathbf{x}}_{j(i)}\left(t^*_{j(i)}\right)$, and $\boldsymbol{\zeta}_{j(i)}\left(t_{j(i)}\right) = \mathbf{0}$, $\dot{\boldsymbol{\zeta}}_{j(i)}\left(t_{j(i)}\right) = \mathbf{0}$. Taking into account some variations in the fractional order $\alpha_{j(i)}$ in Eq (10), we can observe the interesting properties of this force. If $\alpha_{j(i)} = 0$, no viscous term may occur during the contact and all the energy must be due to elasticity. If $\alpha_{j(i)} = 1$, on the other hand, the energy is transfered through the viscous term. Considering such limits we assume variations of this parameter in the range $0 \leq \alpha_{j(i)} \leq 1$. It should be noted that the fractional order $\alpha_{j(i)}$ operates between the surfaces of contacting bodies. This parameter represents the degree of conversion of impact energy into viscoelasticity of the material. With regard to previous considerations presented in [1,2,25] we obtained a model of generalised viscoelasticity operating on fractal surfaces in a topological sense, where the surfaces are rough. Coefficients $c_{j(i)}$ and $k_{j(i)}$ reflect the physical properties of particles during the collision process and the coefficient $\alpha_{j(i)}$ accents the elastic or viscous property.

Several studies presented in this section show experimental evidence that the fractional order reflects the degree to which the induced kinetic energy is converted into material viscoelasticity on the rough surfaces of the contacting particles. The conversion degree $\alpha_{j(i)}$ applied in formula (10) needs some experimental validation in order to reflect the transformation of impact energy into viscoelasticity operating between two rough surfaces during a contact. This will be the further aim and scope of our considerations. Note that the basic models of the repulsive force [3,11,27] do not reflect the roughness of contacting surfaces. In multiparticle contacts, we need to take into account the sum of the force (10) running over all contacting particles $j(i)$.

In the next section we demonstrate how our force operates during a two-particle contact as well as multiparticle contacts. Throughout the collision process, we use a set of equations (1) with the repulsive force (10). The set is numerically solved and the fractional operator inside the repulsive force is represented by a discrete form found in [17].

3 Results and discussion

To illustrate the benefits of our repulsive force, we will present how the force operates under different conditions. We will simulate a particle falling vertically down on to a bottom plate, as shown in Fig. 2. When performing the simulation, the particle falls under gravity and the contact occurs on the plate. When a collision occurs, two schemes of the repulsive force are applied to the motion equation (1), which give the following equations:

$$ m \cdot \ddot{x} + c \cdot \dot{x} + k \cdot (x - r) = -m \cdot g \quad (14) $$

for the linear force (7) proposed by Cundall and Strack [3], and

$$ m \cdot \ddot{x} + c^{\alpha} \cdot k^{1-\alpha} \cdot {}_{t^*}D_t^{\alpha}\,(x - r) = -m \cdot g \quad (15) $$

for our force model presented by formula (10), where r denotes the particle radius and g indicates gravity acceleration. If no collision occurs, we neglect the repulsive force in both Eqs (14) and (15) respectively. Fig. 2a shows the vertical displacement of the particle over time, for different degrees of magnitude of the coefficients k, c. Squares

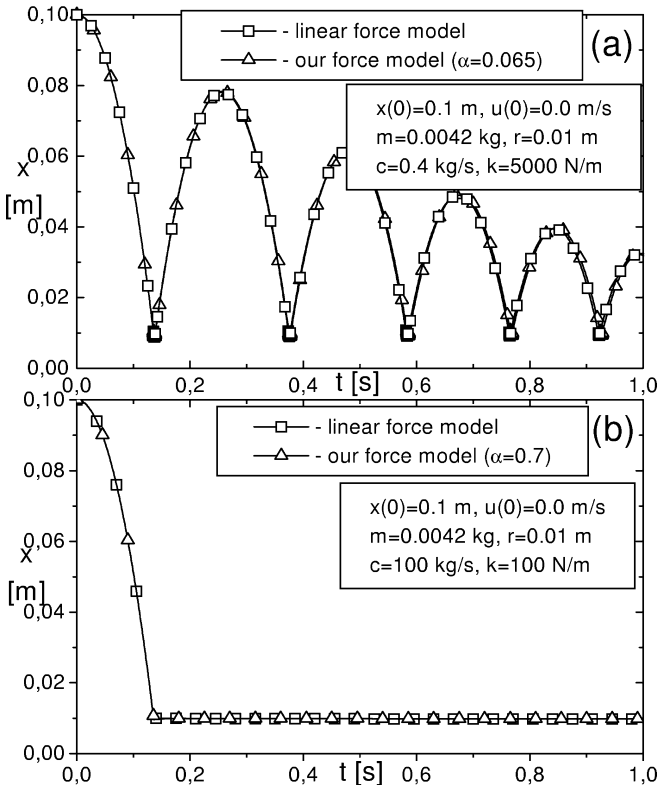

Fig. 2. Comparison of the repulsive forces acting between a particle and the bottom plate for **a** different magnitudes and **b** the same magnitude of coefficients k, c

represent the linear force model (14) and up-triangles indicate our repulsive force (15). For the known initial conditions and physical properties between the particle and the bottom plate as shown on Fig. 2a, we observe good agreement in the results obtained by the linear force equation (7) in comparison to our force equation (10). In this case we estimated the conversion degree α in Eq. (10) as $\alpha = 0.065$.

There is plenty of room available in the conversion degree to simulate other types of behaviour of the particle. Any changes in the coefficients k, c and initial conditions also produce variations in the parameter α. The above example is a comparison of when the values of c and k are chosen to differ by four orders of magnitude from each other and α is set at $\alpha = 0.065$. On the other hand, if c and k are of almost equal magnitude, the parameter α must be increased up to $\alpha = 0.7$ in order to keep good agreement with the linear model. Fig. 2b shows such a situation. There is again plenty of room available in the conversion degree to allow other values of α to be chosen and for other simulations to be made. We can simulate changes in the roughness of the contacting sufraces by varying the value of α. It is not possible to do this with the basic interaction laws [3,11,27]. However, whatever value of α is chosen, the results of a simulation still need to be validated experimentally. Nevertheless, this numerical comparison shows that our interaction law could be adapted using results obtained by the linear force model.

Following on from the results presented by Pournin et al [20] we tried to simulate a set of four identical particles vertically stacked over a bottom plate. Figs 3 and 4 show particle displacements over time depending on the conversion degree α, where the initial distance between neighbouring particles changed from $l_j = 5 \cdot 10^{-4}\ m$ to $l_j = 0\ m$, for $j = 2, ..., 4$. The initial distance between the first particle and the bottom plate is set at $l_1 = 0.03\ m$. For both figures we have $r_j = 0.01\ m$, $m_j = 0.0042\ kg$, $k_j = 5000\ N/m$, $c_j = 0.4\ kg/s$ and $u_j(0) = -0.2\ m/s$, for $j = 1, ..., 4$. As α is increased up to 0.9, the cohesion effect takes place and we can see, on both Figs 3 and 4, that particle trajectories tend to constant values. After collision and with $\alpha = 0.9$, particles stay clustered on the bottom plate. In this particular case the initial distances l_j do not have an influence on the particle trajectories. Therefore, we can say that for higher values of the conversion degree α all impact energy is dissipated and particles stay clustered on the bottom plate. For lower values of α we notice different situations depending on the position of the particle. When $\alpha = 0.01$ and $l_j = 0\ m$ (as shown on Fig. 4) we observe that a greater part of the kinetic energy is transfered to the particle located at the top of the stack in comparison to $\alpha = 0.01$ and $l_j = 5 \cdot 10^{-4}\ m$ (as shown on Fig. 3). When the particle is situated at the bottom of the stack we can see the opposite behaviour to that observed in the previous case.

Next we considered the dynamics of three particles moving in one direction under gravity. Fig. 5 presents particle displacements over time, where the conversion degree α also varies over time. During the first contact between two particles the cohesion effect can be observed using $\alpha = 0.45$. In the next time interval, the particles move as one body until the second contact with the third particle.

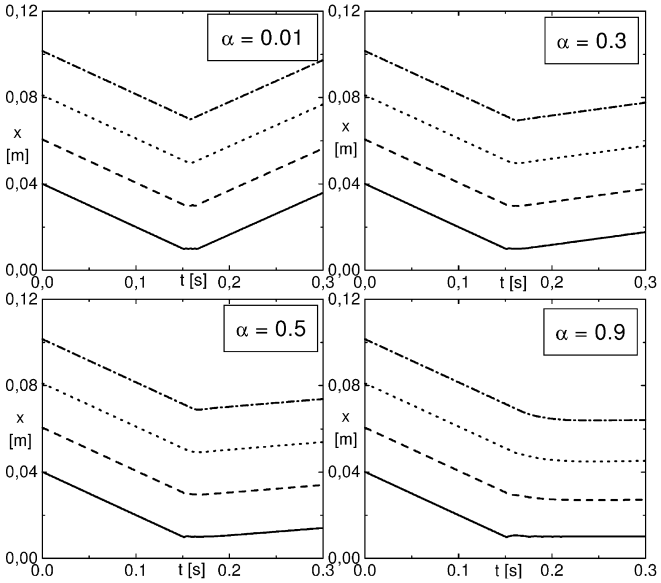

Fig. 3. Particle trajectories vertically stacked over a bottom plate, depending on the values of parameter α, for $l_j = 5 \cdot 10^{-4}\ m$

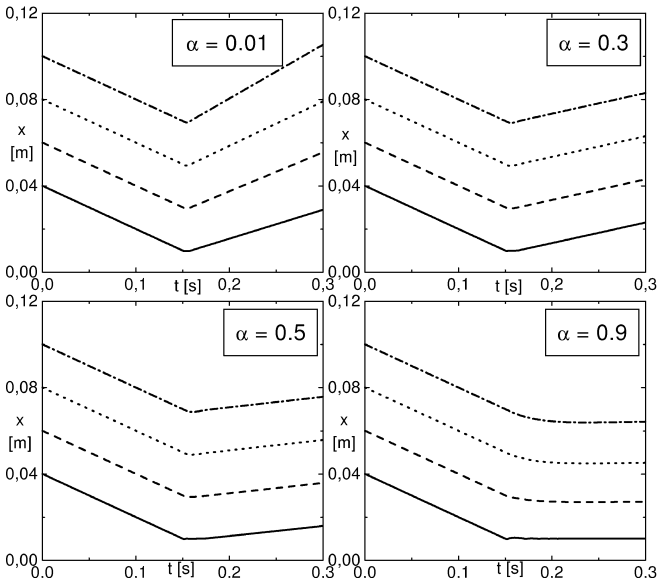

Fig. 4. Particle trajectories vertically stacked over a bottom plate, depending on the values of parameter α, for $l_j = 0\ m$

We can see that the impact energy of the third particle is greater in comparison to the previous one. This directly leads to a decrease in the parameter α, and we set $\alpha = 0.05$. This change breaks the cohesion between the previous two particles, which is shown by the fact that the particle movements are independent of each other. It should be noted that the parameter α can be sensitive to the impact energy.

The next example simulates the dynamics of four particles in two dimensional space for dependent values of parameter α. Fig. 6 presents a situation where a particle with initial velocity $\mathbf{u}_1 = [0, -0.4]\ m/s$ contacts at different moments in time with particles which initially do not move ($\mathbf{u}_j = [0, 0]\ m/s$, for $j = 2, \ldots, 4$). We assumed the

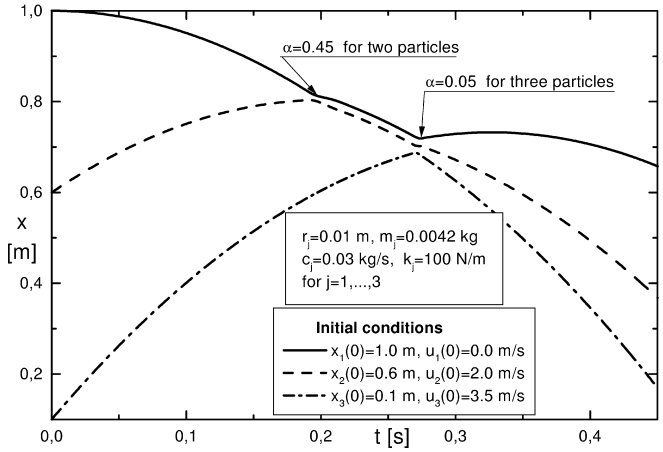

Fig. 5. The influence of the impact energy on changes in the parameter α

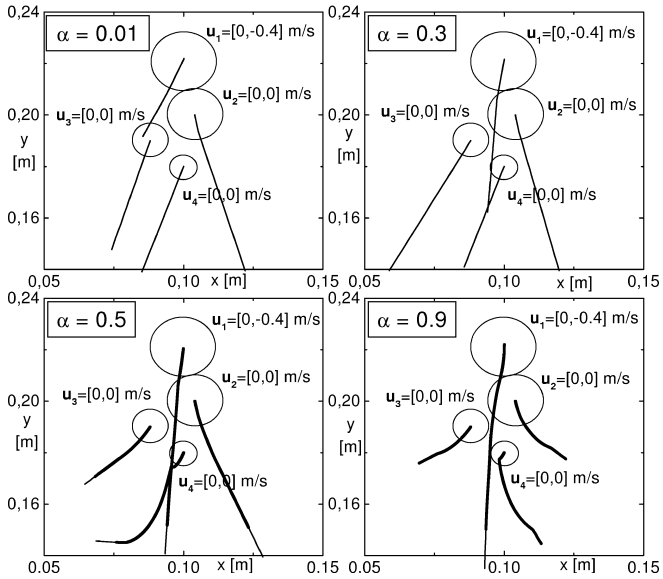

Fig. 6. Behaviour of particle trajectories depending on the values of α

following conditions $r_1 = 0.012\ m$, $m_1 = 7.24 \cdot 10^{-3}\ kg$, $r_2 = 0.01\ m$, $m_2 = 4.19 \cdot 10^{-3}\ kg$, $r_3 = 0.007\ m$, $m_3 = 1.44 \cdot 10^{-3}\ kg$, $r_4 = 0.005\ m$, $m_4 = 0.52 \cdot 10^{-3}\ kg$, and $k_j = 5000\ N/m$, $c_j = 0.1\ kg/s$, for $j = 1 \ldots 4$. This simulation does not reflect real particle behaviour because we neglect tangential forces and particle rotations during particle contacts. We can only show how our force operates in the above conditions. The thin lines represent particle trajectories when particles move separately and the thick lines are common trajectories when particles move as one body. At low values of the parameter α we do not observe these common trajectories, as only binary contacts occur. As the parameter α is increased, up to an upper limit of 0.9, we start to observe common trajectories. This means that in some time intervals the particles move as one body. Moreover, for different values of α we can observe the different lengths of the common trajectories. This arises from the different beginnings of the contact time $t^*_{j(i)}$ between two colliding particles. Comparing particle trajectories, as shown in Fig. 6, we can observe significant changes in particle motions depending on the value of parameter α. Between $\alpha = 0.01$ and $\alpha = 0.3$ linear trajectories occur. For higher variations of the parameter α non-linear trajectories can be observed, this arises from the longer contact time. We can say that the cohesion observed in multiparticle contacts strongly modifies particle motions.

In order to verify the validity of the interaction laws presented here, the energies dissipated at each contact were compared. We used a set of particles np vertically stacked over a bottom plate as shown in Figs 3 and 4 and in [12]. Here we introduce a measure of energy dissipation ε, which is the ratio of the final total kinetic energy over the initial total kinetic energy of a particulate system. Taking into consideration the results presented in [12] we can calculate the energy dissipation as a function of the number of particles np, when $r_i = 0.0015\ m$, $m_i = 1.414 \cdot 10^{-5}\ kg$, $\dot{x}_i = -0.5\ m/s$, and initial distances between neighbouring particles $l_i = 0\ m$, for $i = 1, ..., np$. Gravity is set at 0. Following on from the results presented by Luding et al [12] we assume the same contact time between two colliding bodies $t_c = 10^{-4}s$ and the restitution coefficient $e = 0.949$. These assumptions are necessary to calculate coefficients k, c and k^*, depending on the type of interaction law chosen. Some of the expressions applied to calculate the coefficients for linear and hysteretic laws can be found in [20]. For the non-linear interaction law we performed a computational test to find the values of these coefficients which would allow us to keep the assumed contact time and also the restitution coefficient in a two-particle contact. For the fractional interaction law we assumed the same values of these coefficients as for the linear interaction law. These coefficients represent a collision between two particles or between a particle and a bottom plate, where the mass of the plate is infinite. Fig. 7 shows the ratio of energy dissipation depending on the number of particles np for different interaction laws used in the molecular dynamics method and also in the event driven method [13]. For the basic interaction laws applied in the molecular dynamics method and for the event driven method, we observed the same dependencies as in [12]. This means that all energy should be dissipated for a large number of np. As stated in [12], the energy dissipation

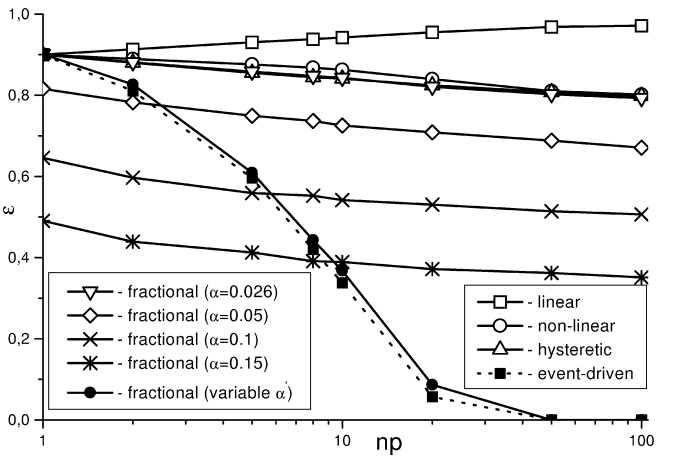

Fig. 7. Total dissipation of energy ε plotted as a function of np for different interaction laws

obtained from the event driven method is close to zero for $np(1-e)$ large. Note that the basic interaction laws are valid for a two-particle contact being completely independent from other contacts which can eventually take place. Nevertheless, in multiparticle contacts we should included mutual dependencies between binary contacts. To this end, the fractional interaction law brings an idea of how to achieve it. First, we considered the fractional law (10) for a steady value of the conversion degree $\alpha_{j(i)}$, for all contacts, as presented on Fig. 7. Note that we obtained similar results between hysteretic and fractional interaction laws for $\alpha = 0.026$. When we increase the value of the parameter α energy dissipation is increased too, but, in this case, we do not restrict previous conditions such as the contact time t_c and the restitution coefficient e. However, small variations in the value of parameter α do not give satisfactory results in comparison to the event driven method, especially when we consider a large number of contacting particles. Above we investigated the fractional formula (10) for contacts which are independent of one another, as in basic interaction laws. Now we shall consider another theoretical situation for a conversion degree which varies depending on the number of particles in a contact with each other. In this case we assume an arbitrary mechanical network composed of contacting particles. Each particle is canfined to contact with only neighbouring particles via hierarchical arrangements of springs and dashpots in order to reflect conversion degree $\alpha_{j(i)}$ between several pairs of particles.

Schiessel and Blumen [23] analysed mechanical fractal networks for the sol-gel transition. They examined the ladder arrangements composed with springs and dashpots related to the gelation process. They proved that the parameter α reflects the structural properties of the system, and especially the conectivity of the network. Moreover, they noted that the network conectivity α depends on the length of the ladder.

In our considerations, the ladder length is represented by the total number of contacting particles np. Therefore, in multiparticle contacts we take into consideration the total conversion degree $\alpha^{'}$, which varies over np. In numerical calculations we substituted $\alpha^{'}$ for $\alpha_{j(i)}$, for each pair of contacting particles restricted to contact with only neighbouring. However, the parameter $\alpha^{'}$ has to be set to reflect the results of known experiments. In this paper, we tuned $\alpha^{'}$ in order to reflect quantitatively the results obtained from the event driven method [13]. Fig. 7 shows such a comparison between the event driven method and the fractional interaction law, where the filled squares indicate the event driven technique, and the filled circles represent the fractional interaction law (10) with the total conversion degree $\alpha^{'}$. We obtained quantitatively good results for $\alpha^{'} \sim (np)^{0.468}$. However, it should be noted that in the event driven method the inelastic collapse phenomenon [13] occurs, where the whole energy of the system is dissipated. So we cannot estimate $\alpha^{'}$ by direct comparison with the event driven technique. Instead we require experimental data involving more than one contact. This data will provide measures that allow analytical links to be made between the experiment and the model parameters.

4 Conclusions

We have proposed and discussed a novel model of the repulsive force acting between particles in a normal direction. This model allows us to control dynamically the transfer and dissipation of energy in granular media. Our formula is defined under fractional calculus, where a fractional derivative accumulates the whole history of the virtual overlap over time in weighted form. This feature, in comparison to the known models of the repulsive force, is a generalisation. We then discussed and illustrated the basic properties of the repulsive force. Some of the parameters of this model may still need to be tuned, as for example, the parameter α in order to reflect the conversion degree of colliding particles. Moreover, a sensitivity study of the parameter α depending on the impact energy needs to be done. Nevertheless, this approach allows us to perform simulations of arbitrary multiparticle contacts and granular cohesion dynamics.

References

1. R. L. Bagley & P. J. Torvik, A theoretical basis for the application of fractional calculus to viscoelasticity. J. Rheol., 27 (1983), p. 201–210
2. A.-L. Barabási & H. E. Stanley, Fractal concepts in surface growth. Cambridge University Press, Cambridge, 1995
3. P. A. Cundall & O. D. L. Strack, A discrete numerical model for granular assemblies. Geotechnique, 29 (1979), p. 47–65
4. E. A. Eklund et al., Submicronscale surface roughening induced by ion bombardment. Phys. Rev. Lett. 67 (1991), p. 1759–1762
5. D. Gidaspow, Multiphase flow and fluidization. Continuum and kinetic theory descriptions. Academic Press, San Diego, 1994
6. D. Greenspan, Discrete Models. Addison-Wesley, London, 1973
7. R. Hilfer (eds), Applications of fractional calculus in physics. World Scientific, Singapore, 2000
8. R. W. Hockney & J. W. Eastwood, Computer Simulation Using Particles. McGraw-Hill, 1981
9. K. L. Johnson, Contact mechanics. Cambridge University Press, Cambridge, 1985
10. M. Kardar & J. O. Indekeu, Wetting of fractally rough surfaces. Phys. Rev. Lett. 65 (1990), p. 662–672
11. G. Kuwabara & K. Kono, Restitution coefficient in a collision between two spheres. Japanese Journal of Applied Physics, 26 Part 1 (1987), p. 1230–1233
12. S. Luding, E. Clément, A. Blumen, J. Rajchenbach & J. Duran, Anomalous energy dissipation in molecular dynamics simulations of grains. Phys. Rev. E, 50 (1994), p. 4113–4122
13. S. McNamara & W. R. Young, Inelastic collapse and clumping in a one dimensional granular medium. Phys. Fludis A, 4 (1992), p. 496–504
14. H. G. Matuttis, S. Luding & H. J. Herrmann, Discrete element methods for the simulation of dense packings and heaps made of spherical and non-spherical particles. Powder Technology, 109 (2000), p. 278–292
15. R. Metzler et al., Relaxation in filled polymers. J. Chem. Phys., 103(16) (1995), p. 7180–7186

16. R. M. Nedderman, Statics and dynamics of granular materials. Cambridge University Press, Cambridge, 1992
17. K. B. Oldham & J. Spanier, The fractional calculus. Theory and applications of differentiation and integration to arbitrary order. Academic Press, New York, 1974
18. P. Pfeifer et al., Multilayer adsorption on a fractally-rough surfaces. Phys. Rev. Lett. 62 (1989), p. 1997–2000
19. T. Pöschel et al., Scaling properties of granular materials. In P. A. Vermer et al. (eds), Continuous and discontinuous modelling of cohesive-frictional materials. Lecture Notes in Physics 568 (2001), Springer-Verlag, p. 173–184
20. L. Pournin & Th.M. Liebling, Molecular dynamics force models for better control of energy dissipation in numerical simulations of dense granular media. Phys. Rev. E, 65 (2001), p. 011302-1-011302-7
21. D. C. Rapaport, The art of molecular dynamics simulation. Cambridge University Press, 1995
22. S. G. Samko, A. A. Kilbas & O. I. Marichev, Fractional Integrals and Derivatives. Theory and Applications. Gordon and Breach, Amsterdam, 1993
23. H. Schiessel & A. Blumen, Mesoscopic pictures of the sol-gel transition: Ladder models and fractal networks. Macromolecules, 28 (1995), p. 4013–4019
24. H. Schiessel, Chr. Friedrich & A. Blumen, Applications to problems in polymer physics and rheology. In R. Hilfer (eds), Application of fractional calculus in physics. World Scientific, Singapore (2000), p. 331–376
25. H. Schiessel, R. Metzler, A. Blumen & T. F. Nonnenmacher, Generalized viscoelastic models: their fractional equations with solutions. J. Phys. A: Math. Gen., 28 (1995), p. 6567–6584
26. P. A. Vermer et al. (eds), Continuous and discontinuous modelling of cohesive-frictional materials. Lecture Notes in Physics 568, Springer-Verlag, 2001
27. O. R. Walton & R. L. Braun, Viscosity, granular-temperature and stress calculations for shearing assemblies of inelastic frictional disks. J. Rheol., 30 (1986), p. 949–980